

Long-Term Shrinkage Cracking Behavior in Fully Restrained Concrete Panels Reinforced with GFRP Bars



Wei Wang¹ and John J Myers^{2*}

¹Department of Civil, Architectural and Environmental Engineering, Missouri University of Science and Technology, USA

²Department of Civil, Architectural and Environmental Engineering, Missouri University of Science and Technology, USA

Submission: February 19, 2018; **Published:** May 04, 2018

***Corresponding author:** John J Myers, Department of Civil, Architectural and Environmental Engineering and Associate Vice Provost and Dean of College of Engineering and Computing, Missouri University of Science and Technology, Rolla, MO, USA, Email: jmyers@mst.edu

Abstract

An experimental program was developed to investigate the effects of restrained shrinkage and temperature changes on the cracking behavior in fully restrained concrete panels reinforced with glass fiber reinforced polymer (GFRP). An analytical model was refined based on original work by Gilbert [1]. It was modified and applied to predict cracking behavior for each GFRP panel. One steel (panel P-1) and five GFRP reinforced panels (panels P-2 through P-6) with varying widths were constructed by Branham and Myers [2]. Reinforcement ratios were designed according to ACI 318 [3] and ACI 440 [4] respectively. Six panels were subjected to a Midwest US exterior environment for almost seven years. There were three stages to study cracking behavior of these panels. The first and second stages were undertaken and completed by different researchers. In this work, the experimental results were presented in terms of cracking pattern, crack width, and cracking spacing for each panel over a period of 2400 days after fabrication. The maximum crack widths and the final average crack widths were compared in the six panels. The experimental values compared with the analytical results by using modified Gilbert's model. The comparison illustrated a relatively small error between model's results and data measured. A refinement to Gilbert's model was proposed for GFRP reinforced concrete panels.

Keywords: Fully restrained concrete panel; Glass fiber reinforced polymer (FRP); Cracking behavior; Cracking pattern; Crack width; Cracking spacing; Shrinkage and temperature reinforcement

Abbreviations: GFRP: Glass Fiber Reinforced Polymer; RC: Reinforced Concrete; SRH: Shrinkage-Reducing Admixtures; UPV: Ultrasonic Pulse Velocity; RCPT: Rapid Chloride Permeability; CTE: Coefficients of Thermal Expansion

Introduction

Shrinkage of concrete is the reduction of volume caused by loss of water during the drying process (drying shrinkage) and also by chemical reactions of hydration of cement paste (endogenous shrinkage or autogenous shrinkage). Concrete structures are free to contract if shrinkage is not restrained. As a result, shrinkage has little consequence. However, some level of restraint is common in concrete structures. As an example, the bonded reinforcement in concrete structures provides restraint to shrinkage. The reinforcement imposes a tensile force on the concrete at the level of the reinforcement when the concrete shrinks. At the same time, the reinforcement produces an equal and opposite tensile force on the concrete at the level of the reinforcing bars. This internal tensile restraining force is often important enough to cause cracking of concrete members. In addition, connections and/or boundary conditions provide restraint to shrinkage if a concrete member is connected to other parts of the structure or to the foundation. The tensile restraining force can develop rapidly with time at the restrained ends of the member, which results in cracking. Thin floor slabs and walls in

buildings are particularly prone to significant cracking resulting from restrained shrinkage and temperature changes [5].

In addition, reinforced concrete (RC) structures with high surface-to-volume ratios such as bridge deck slabs, concrete pavements, and parking garages form easily transverse cracks due to restraint to shrinkage of concrete. Because bridge deck slabs are typically much longer in one direction than the other, volumetric changes of concrete due to shrinkage and thermal changes are more pronounced in the longitudinal direction. In slab-on-girder bridges, the girders and continuity of slabs restrain the movement of deck slabs due to shrinkage and thermal changes, which induces stresses that result in transverse cracks [6,7]. Shrinkage is greatest at the surface of a concrete member when exposing to drying environment, and decreases gradually towards the interior of the member. The resulting differential shrinkage across the member's cross section produces tensile stresses near the drying surface that may lead to surface cracking [5]. In restrained concrete members, cracks generally penetrate over the full depth of members' cross sections. The width of a

crack depends on the quantity, orientation, and distribution of the reinforcing bars crossing the crack. The bond characteristics between concrete and reinforcement bars also can influence the width of the crack.

Full-depth cracks are generally considered the most severe form of bridge deck slab cracking. Due to the use of deicing salts, the chlorides penetrate the concrete and reach the steel reinforcement through cracks. They will attack the concrete surrounding the reinforcing bars, which makes the pH value of the concrete drop. They serve as the catalyst that breaks down the protective alkalinity layer around the reinforcing bars and allow oxygen and moisture to initiate the corrosion process. The corrosion of steel reinforcement can cause some undesirable consequences for reinforced concrete. Therefore, the non-corrodible glass fiber reinforced polymer (GFRP) bars have been applied due to their lower cost, higher tensile capacity, and lower weight to decrease the corrosion problem of conventional reinforcing steel. GFRP bars, however, have relatively lower modulus of elasticity than steel bars, which can result in wider cracks in concrete structures reinforced with GFRP bars. Although GFRP bars cannot be corroded like steel bars, GFRP-RCs are still susceptible to other forms of deterioration due to harsh environments involving deicing chemicals, sulfate salts and alkalis, which can readily infiltrate concrete through cracks [8].

There are extremely limited data that are available on long-term restrained shrinkage cracking field studies of RC members particularly members with GFRP. Therefore, this work examines crack patterns of in concrete panels reinforced with GFRP bars during seven years including the effect of panel size with low GFRP longitudinal reinforcement ratio on long-term shrinkage cracking under field environment to find a more reasonable reinforcement ratio of GFRP-reinforced concrete for shrinkage and temperature reinforcement, and to compare crack width using a published analytical model [1].

Previous Works

The objective of the original study was to investigate the appropriateness of the ACI 440.1R code in designing secondary reinforcement for GFRP. An experimental program was developed to investigate the effects of temperature and shrinkage of the concrete on crack widths in concrete panels reinforced with GFRP bars. Six panels were constructed; one steel control and the ACI 318 lower limit for secondary reinforcement, and five subsequent panels reinforced with GFRP bars at varying reinforcement ratios. A finite element analysis was also done to further investigate the effects of temperature and shrinkage on the RC panels. It was concluded from experimental testing that the ACI 440.1R code was overly conservative in estimating the amount of secondary reinforcement needed to control the effects of temperature and shrinkage [2].

The second stage of this overall program was performed approximately one-and-a-half years after the finish of the first

period. Its objective was to determine how crack patterns have changed in the time since the end of the previous study. In addition, this second study was used to determine whether the conclusions drawn from the first portion of the experiment still seemed to apply. This study supported the plausibility of using GFRP reinforcement in place of steel [9]. Since GFRP does not have problems with corrosion, unlike steel, larger crack widths may be tolerated, as long as aesthetics is not a concern.

Early-age cracking of concrete bridge deck slabs, typically resulted from autogenous shrinkage, drying shrinkage, and thermal changes, could produce several disadvantageous influences on long-term behavior and durability. As water is consumed by the ongoing hydration process, the voids empty, and capillary stresses are generated resulting in a volumetric shrinkage. Autogenous shrinkage is concrete volume change occurring without moisture transfer to the environment [10]. There are enough water in concrete voids to provide hydration reaction, and stresses associated with autogenous shrinkage do not develop when the ratio of water to cement or cementitious material (w/cm) exceeds 0.42 [11]. In this paper, w/cm of the concrete was 0.5, the autogenous shrinkage, therefore, was not major reason to cause the concrete panels volume change.

Thermal changes of concrete from hydration processes can increase the early-age cracking tendency of freshly placed concrete bridge decks. Higher thermal stresses in fresh concrete would produce when increasing placement and curing temperature. The early-age cracking of bridge deck concrete occurs when the thermal stresses exceed its tensile strength [12]. The ambient temperature and humidity variations mainly control the shrinkage of concrete. Transverse cracking of concrete bridge deck slabs commonly occurred in bridge superstructures after concrete hardens [6]. In addition, reinforcement bars create internal restraint and can limit transverse crack width as shrinkage and thermal changes generated tensile stress in concrete that exceeded the tensile strength of concrete. However, the internal restraint of reinforcement can be ignored or is negligible compared with external restraints like adjoining members or the continuity of concrete bridge deck slabs that could cause restrained shrinkage cracking [13].

Restrained shrinkage cracking of concrete bridge deck slabs has become a common problem in the United States. Restraint to shrinkage can lead to cracking that is time-dependent, and gradually decays the positive influences of tension stiffening of concrete. Consequently, it makes existing cracks be wider in concrete members [14]. According to a study carried out by Krauss and Rogalla [6], more than 100,000 bridges in the U.S. faced early-age shrinkage cracking problems. Qiao et al. [15] studied the main factors of the early-age cracking in the bridge decks.

According to previous studies [16-18], these causes included low humidity and hot weather, low water-cementitious material ratio, improper mix design with high cement content or high

quantity of water, restraint from deep longitudinal girders and their connections, low tensile strength of concrete, high modulus of elasticity of concrete, low creep properties, temperature differential between the newly-placed deck and supporting girders with different shrinkage rates, and high curing temperatures. In order to evaluate the causes that affected restrained shrinkage cracking of concrete, they conducted restrained shrinkage ring tests. Finally, shrinkage-reducing admixtures (SRA) were recommended to minimize early-age shrinkage cracking. In addition, larger sizes of aggregates in concrete were also proposed to reduce shrinkage. Gilbert [1] considered shrinkage cracking in fully restrained reinforced concrete (RC) members subjected to direct tension force resulted from dry shrinkage. The mechanism of shrinkage tension cracking was discussed. A reasonable analytical approach that determined average crack width, spacing of cracks, and final stresses in reinforcing bars and concrete was developed.

Nejadi and Gilbert [19] found that shrinkage deteriorated the transition zone between steel and concrete. As a result, the bond at the steel-concrete interface lessened gradually with time. Finally, the distance so on each side of the crack, which the concrete and steel stresses were no longer affected by the occurrence of the crack, increased progressively with time. Therefore, for long-term shrinkage cracking study, the value of α should be multiplied by 1.33.

Nejadi and Gilbert [5] built eight longitudinally restrained concrete slabs reinforced with steel bars with different reinforcement layouts. The slabs were anchored at their ends by concrete blocks. These concrete blocks provided the restraint to shrinkage of slabs. They were considered to be immovable previously. These concrete members, however, also shrank with time. Therefore, a relative movement (Δu) of supports was considered in theoretical analysis. The ultimate average crack width, spacing of cracks, final stress of reinforcement in crack, and ultimate concrete stress away from crack were measured. Finally, they were compared with the theoretical 0072 results using the analytical model developed by Gilbert. They found that the final crack width, the crack spacing, and steel stress at each crack reduced with an increase in the steel area, and the concrete stress away from a crack increased with increasing the reinforcement ratio of concrete slabs. The experimental and theoretical values were similar. However, they considered that crack width and crack spacing could not be predicted with any great accuracy using an analytical model because cracking in restrained reinforced concrete members was extremely variable.

Early-age cracking of bridge deck slabs can increase penetration of harmful elements like chloride ions from deicing salts, which serve as the catalyst that breaks down the protective alkalinity layer around the reinforcing bars and allow oxygen and moisture to initiate the corrosion process. The use of fiber reinforced polymer (FRP) bars can improve corrosion of steel due to their higher resistance to corrode. Ghatefar et

al. [20] performed an experimental study on effect of different longitudinal reinforcement ratio (0.30, 0.50, 0.70 and 1.1%) on transverse early-age cracking of GFRP-RC bridge deck slabs (2,500mm long x 765mm wide x 180mm thick). These slabs were fixed at their ends by 1,473 x 1,000 x 1,200mm concrete blocks, which were fastened to the laboratory strong floor before casting. Crack width and strains in GFRP bars and concrete were measured. At the same time, a published model that Gilbert predicted restrained shrinkage cracking was utilized to calculate ultimate GFRP bar stress at the crack and crack width. They found that the average crack width at mid-span and strain in GFRP bars and concrete decreased when increasing reinforcement ratio. The measured final shrinkage crack width and stresses in GFRP bars were compared with the results of Gilbert analytical model. The errors were within 16%. The coefficient of α should be modified to 0.8 instead of 1.33 when GFRP bars replaced steel.

Ghatefar et al. [21] focused on the effect of different environmental conditions on early-age restrained shrinkage cracking of GFRP-RC bridge deck slabs with the reinforcement ratio of 0.7% recommended by the Canadian Highway Bridge Design Code 2006 (CHBDC 2006) for concrete bridge deck slabs reinforced with GFRP bars. The same dimension of concrete slab as that of Ghatefar et al. [20] was used. Two slabs reinforced with GFRP and steel bars were investigated under the laboratory condition. And two specimens reinforced with GFRP bars were experimented under freezing-thawing and wetting-drying conditions. Crack widths, spacing of cracks, and strains in concrete and reinforcing bars were measured. Ultrasonic pulse velocity (UPV), Rapid chloride permeability (RCPT) tests and micro structural analysis were used to investigate degradation of concrete exposed to cyclic conditions. They found that the minimum reinforcement ratio of 0.7% satisfied the serviceability requirements. The results of material tests showed that there was some degradation of concrete exposed to cyclic conditions. At the same time, the theoretical model developed by Gilbert was used to predict crack widths and stresses in GFRP bars. The results illustrated that the experimental results were similar with those predicted by Gilbert analytical model within 17% error.

Although numerous researchers have studied the behavior of shrinkage cracking of concrete elements reinforced with steel and GFRP bars, their studies focused on early-age cracking behavior of GFRP concrete members. There is very limited data to evaluate restrained shrinkage cracking of FRP-RC members under long-term exposure to field environment. Further study, therefore, is needed in this area. This paper contributed an experimental study that investigated the effect of low longitudinal (secondary) GFRP reinforcement ratio on long-term shrinkage cracking in fully restrained concrete element exposed to natural environment. At the same time, a model that was developed by Gilbert initially was modified to predict the cracking behavior for GFRP panels.

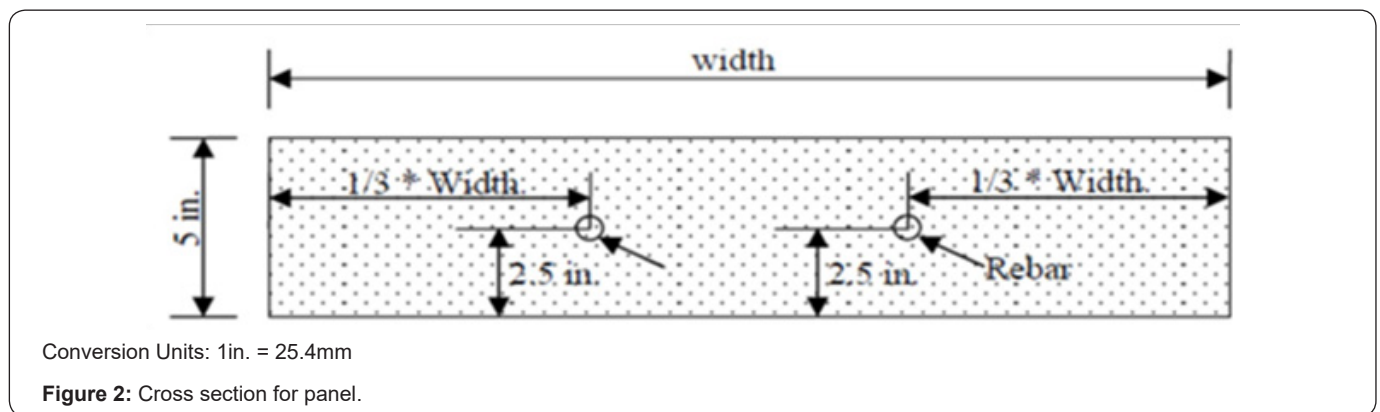
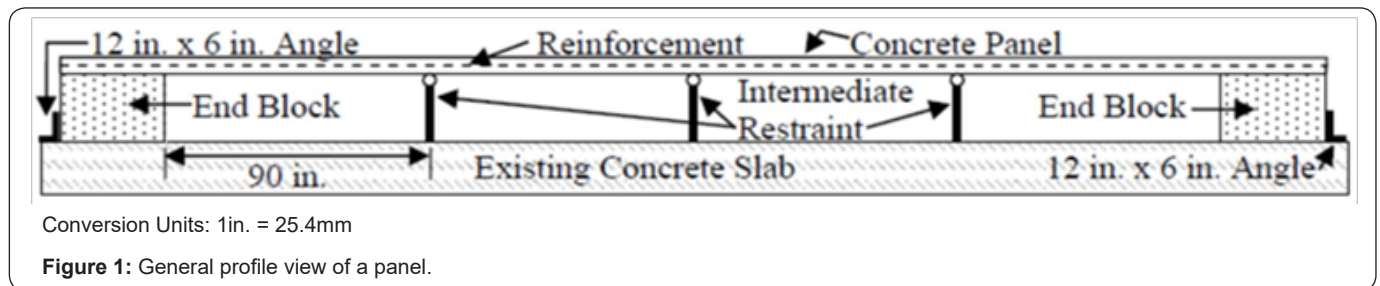
Experimental Programs

General

The initial study concentrated on two specifications that set limits and recommendations for design methods when dealing with cracking of reinforced concrete. ACI 318 "Building Code Requirements for Structural Concrete" Section 7.12 sets temperature and shrinkage specifications for concrete reinforced with conventional steel. ACI 440.1R "Code Recommendations for FRP" Section 10 specifies temperature and shrinkage recommendations for concrete reinforced with fiber reinforced

polymers. During the first portion of the experiment (days one through 203), crack patterns were recorded and a related creep and shrinkage study was done on the concrete mix. During the second phase of testing (at 762 days), crack patterns were again recorded to compare to the original data. In the final period of this research, crack patterns and crack widths were compared to the previous results after seven years when the panels were constructed in this paper. Meanwhile, the analytical model developed initially by Gilbert was used to predict the final average crack widths and average spacing of crack for the panels reinforced with GFRP bars.

Experimental test setup



In this study, six concrete panels with different widths were made. The first specimen was reinforced with 60ksi (413.7MPa) embedded steel reinforcing bars. The latter five specimens were reinforced with 110ksi (758.4MPa) embedded GFRP reinforcement. The panels were cast at a 30 feet (9.14m) span consisting of four spans of 7.5 feet (2.286m). The depth of each panel was 5 inches (127mm). The intermediate supports with #10 GFRP bars, each at 7.5 feet (2.286m), were constructed to attain a roller restraint, so that these panels could move freely in the lateral direction. In order to complete full restraint situation

the panels were detailed with restrained end reinforced concrete blocks (2 feet (0.610m) wide by 3 feet (0.914m) long by 2 feet (0.610m) deep). These blocks restrained sufficiently the continuous span panels. A typical profile view of a panel is illustrated in Figure 1. Reinforcing bars were placed in center of the panels. Figure 2 shows cross section and reinforcement placement for panel.

Table 1 reports the panels ID, reinforcement types and panels' size. All panels were cast outside and left exposed to the field environment for even years.

Table 1: Summary of panels.

Panel	Reinforcement Type	Reinforcement Area (mm ²)	Length (mm)	Width (mm)	Depth (mm)
P-1	Steel	142	9144	621	127
P-2	GFRP	168	9144	734	127
P-3	GFRP	168	9144	604	127
P-4	GFRP	168	9144	402	127

P-5	GFRP	168	9144	302	127
P-6	GFRP	168	9144	242	127
Conversion Units: 1 in. = 25.4 mm, 1in.2 = 645.16 mm ²					

Concrete properties

The panels were cast using a 4,000psi (27.58MPa) mix design. The concrete compressive strength tests were determined at

different ages as shown in Table 2. The concrete was delivered mixed to the cast site.

Table 2: Compressive strength concrete (Branham and Myers 2006).

Concrete Ages (Days)	Average Compressive Strength (psi)
1	1840
7	3530
14	3560
21	3820
28	3850
Conversion Units: 1 psi = 0.0069 MPa	

Reinforcement properties

Each panel consisted of four reinforcement bars. Two reinforcement bars made up the reinforcement section for each side of the panel. The reinforcement was spaced at 1/3 the width of the beam. The reinforcement was spaced 1 inch (25.4mm)

from the back of the end block, and had a splice length of 4 feet 2 inches (1.27 m) at mid-span of the panel. All reinforcement bars were No. 3 in size. The steel tensile coupons were tested. Table 3 shows the steel properties and size respectively. No. 3 GFRP bars were used. The properties of GFRP bars published by Hughes Brothers were illustrated in Table 4.

Table 3: Steel reinforcement (Branham and Myers 2006).

Bar Number	Diameter (mm)	Area (mm ²)	Grade	fy (MPa)	fu (MPa)
3	9.53	71	40	344.9	519.5
Conversion Units: 1 in. = 25.4 mm, 1in2 = 645.16 mm ²					

Table 4: GFRP reinforcement (Branham and Myers 2006).

Bar Number	Diameter (mm)	Area (mm ²)	ffu (MPa)	Ef (MPa)
3	9.53	84.3	758.4	4.08 x 10 ⁴
Conversion Units: 1 in. = 25.4mm, 1in.2 = 645.16mm ²				

Data acquisition

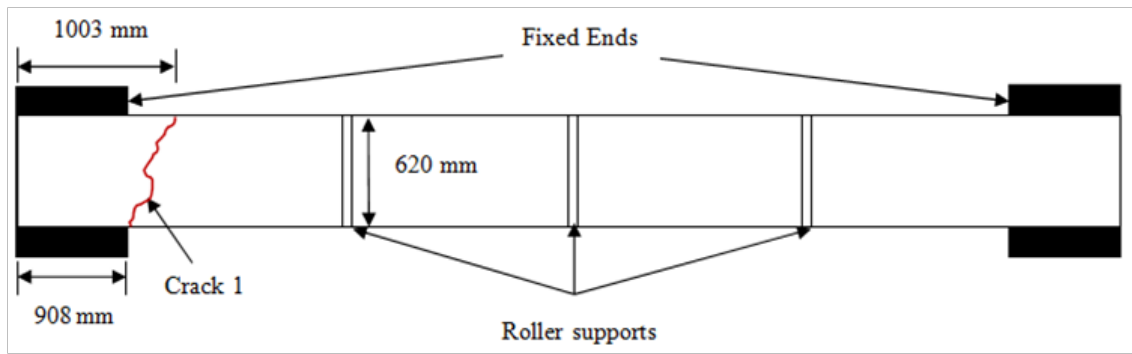
The final crack widths were measured with a crack scope (CS-100 Crack Scope manufactured by PEAK). The crack scope had a 25X magnification, and measured to an accuracy of 0.004 inch (0.1mm). The lens of the crack scope stands 1 inch (25.4mm) from the surface of the concrete, and has manual focus for better clarity in viewing the crack. On the top of the panels, five measurements were taken along the length of each crack. The five measurements were then averaged for the final average crack width.

Experimental Results and Discussion

Crack patterns of the panels

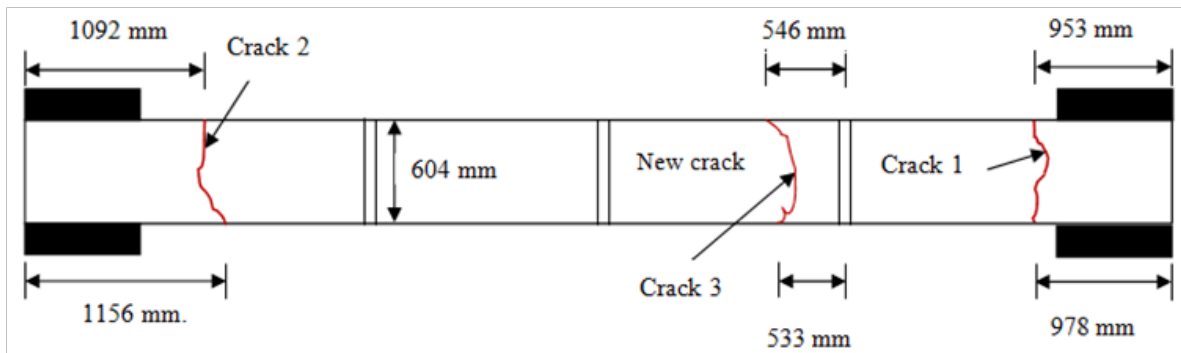
Because there were three times as much concrete that tended to shrink in the longitudinal direction than in the

transverse direction [7], restrained shrinkage cracks developed in transverse direction of the panels in order to relieve the larger tensile stress due to restrained end blocks in the longitudinal direction. Cracks propagated over the full depth of the panels when observing cracking in the panels after exposure of seven-year field environment. These cracks appeared at or near restrained end supports or intermediate supports, as can be seen in the following figures. Also, the majority of the cracks appeared in the original and second study period (762 days); only 3 new cracks were observed in panels P-3, P-4 and P-6, respectively in final study phase. There was still only one crack in panel P-1 during these years. When observing the crack patterns for these panels, it should be noted that the center support for panel P-2 was damaged, which may have affected the results somewhat. The following Figures 1 through 6 illustrate the various crack patterns and locations of the cracks observed in last stage.



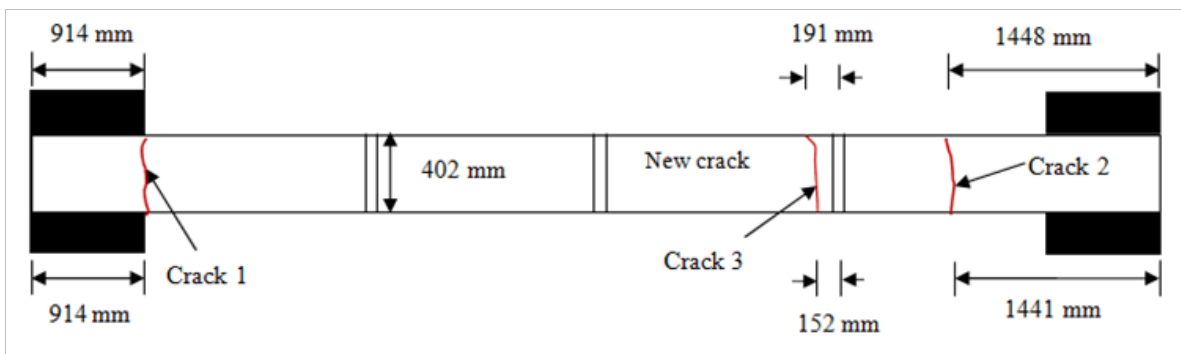
Conversion Units: 1in. = 25.4mm

Figure 3: Panel P-2 (GFRP, $\rho = 0.18\%$).



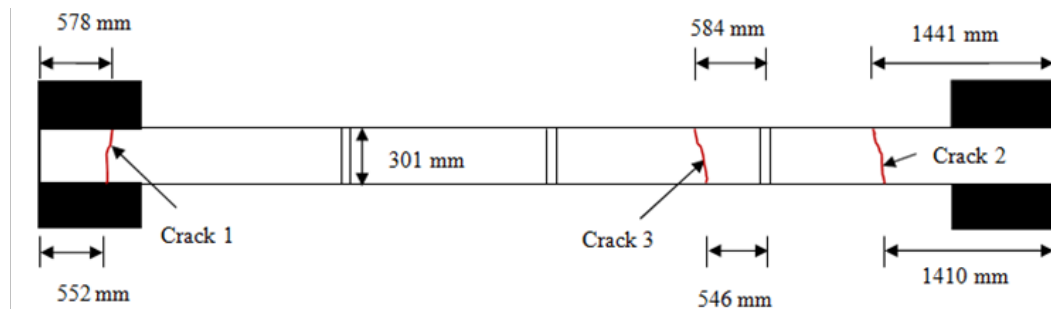
Conversion Units: 1in. = 25.4mm

Figure 4: Panel P-3 (GFRP, $\rho = 0.22\%$).



Conversion Units: 1in. = 25.4mm

Figure 5: Panel P-4 (GFRP, $\rho = 0.33\%$).



Conversion Units: 1in. = 25.4mm

Figure 6: Panel P-5 (GFRP, $\rho = 0.44\%$).

Because this study involved GFRP reinforced concrete panels at the secondary reinforcement level (low levels of reinforcement), the GFRP bars on panels 2 through 6 were subjected to sustained stress levels throughout the exposure conditioning due to the dead load weight of the panels. The maximum positive and negative moments due to self-weight of concrete and predicted cracking moments of these panels are illustrated in Table 5. The distributed moment and shear stresses were maximum values at the restrained concrete supports and interior roller supports on these panels, the maximum tensile stresses occurred at the interior and exterior supports, and were equal. In addition, axial restraining forces $N(t)$ induced by the restrained shrinkage and temperature changes of these concrete panels caused the highest level of tensile stress at the exterior support of the panel. This could explain that all six of the tested panels cracked at or near the exterior and interior supports.

From Table 5, it should be noted that self-weight of these GFRP panels cannot alone induce cracking of concrete because the cracking moments are greater than the maximum moments caused by self-weight. It can be concluded that these panels were not subjected to significant bending in which restraint was provided to the longitudinal movement induced by shrinkage and temperature changes. In general, these cracks are called direct tension cracks because they were induced by axial tension force rather than flexural tension. Restrained drying shrinkage, therefore, was a major factor inducing cracking of these panels. When the concrete panels shrank, the axial tensile restraining forces developed with time. As a result, cracks formed in these concrete panels due to restraint of end concrete blocks that restrained free volumetric changes of the panels when the concrete stress caused by $N(t)$ at a particular cross section first reached the direct tensile strength of concrete.

Table 5: Sustained maximum moments due to self-weight and cracking moments.

GFRP Panel	Max. Negative Moment (N-m)	Max. Positive Moment (N-m)	Cracking Moment (N-m)
Panel 2	-960.9	480.4	6,362.00
Panel 3	-786.3	393.1	5,205.30
Panel 4	-524.1	262.1	3,470.20
Panel 5	-393.1	196.6	2,593.90
Panel 6	-314.3	157.2	2,083.40

Conversion Units: 1in. = 25.4mm; 1 lb. = 0.454kg

Crack widths and changes over time

During the initial study period, the first sign of cracking observed was at 13 days. There were four panels (panels P-2, P-4, P-5, and P-6) that cracked 13 days after casting. Each panel appeared one crack that extended the full width of the panel and propagated over the full depth of the panel. The crack widths were 0.0085 inch (2.159mm), 0.0046 inch (0.11684mm), 0.00197 inch (0.05004mm), and 0.00197 inch (0.05004mm) respectively. The crack in panel P-1 (Steel, $\rho=0.18\%$) was first observed 28 days after casting and measured 0.000656 inch (0.01666mm) in width. The first crack in panel P-3 was observed 19 days after casting. This crack width was 0.00394 inch. Panel P- 6 developed a second crack at 64 days on the opposite side of the first crack. This second crack in P-6 measured 0.00197 inch (0.05004mm). A second crack was observed in panel P-3 at 203 days from casting. This crack had a width of 0.00197 inch (0.05004mm). At 203 days a second crack was also observed in panel P-5, the width was 0.00197 inch (0.05004mm) in width. This second crack in panel P-5 was on the opposite side of its first crack [2].

During the second study period (at 762 days), two new cracks in panel P-2 were observed at second intermediate roller support and near right fixed end block, respectively. Panel P-4 appeared a new crack that was closed to left exterior support. Panel P-5 developed a new crack near the third intermediate roller restraint. There were no new cracks in other panels.

Average crack widths of these panels in this stage were greater than those in the first phase study. The maximum average crack width was 0.0237 inch (0.602mm) that was observed in panel P-2. The minimum average crack was observed in panel P-5, the crack width was 0.0053 inch (0.135mm), as illustrated in Table 6. During the original study period, crack measurements ranged in width from 0.00026 inch (0.0066mm) to 0.0085 inch (0.216mm). Crack widths for the second study period ranged from 0.004 inch (0.102mm) to 0.039 inch (0.991mm), a 93.3% and 78.3% increase from the original minimum and maximum, respectively [9].

During the final observation, the average crack widths for panels P-1 through P-6 were higher than the values measured in the second study period. The maximum average crack was formed in panel P-2, the width was 0.0587 inch (1.491mm). Panel P-5 appeared the minimum average crack of 0.0289 inch (0.734mm). Table 6 illustrates the ultimate average crack widths and crack numbers in different study period.

Panel P-1 (Steel, width = 620mm) appears a relatively small final crack width when comparing these results for these six panels, as shown in Table 6-8. Due to higher stiffness of steel reinforcing bars than GFRP reinforcement, higher internal tensile stresses in panel P-1 will develop due to internal restraint against concrete shrinkage or temperature variations, which leads to a relatively small ultimate average crack width in panel P-1. At the same time, panel P-2 illustrates the maximum average

crack width comparing with those results of panels P-3, P-4, P-5, and P-6. The reason is that the dimension for panel P-2 is the biggest, and the reinforcement ratio of this panel is the smallest than those counterparts of the other GFRP panels.

Table 6: Average Crack Width and Crack Numbers at Different Time.

Panel	At 203 Days		At 762 Days		At 2400 Days	
	Ave. Crack Width (mm)	Crack No.	Ave. Crack Width (mm)	Crack No.	Ave. Crack Width (mm)	Crack No.
P-1	0.05	1	0.193	1	0.782	1
P-2	0.1	1	0.602	3	1.491	3
P-3	0.075	2	0.178	2	0.889	3
P-4	0.083	1	0.188	2	0.892	3
P-5	0.075	2	0.135	3	0.734	3
P-6	0.067	2	0.168	2	0.907	3

Conversion Units: 1 in. = 25.4mm

Table 7: Maximum Crack Widths at Different Time (mm).

Panel	1-203 (day)	762 (day)	2400 (day)
P-1	0.0668	0.406	0.991
P-2	0.217	0.991	2.21
P-3	0.133	0.305	1.702
P-4	0.15	0.305	1.397
P-5	0.133	0.254	1.092
P-6	0.117	0.254	1.854

Conversion Units: 1 in. = 25.4 mm

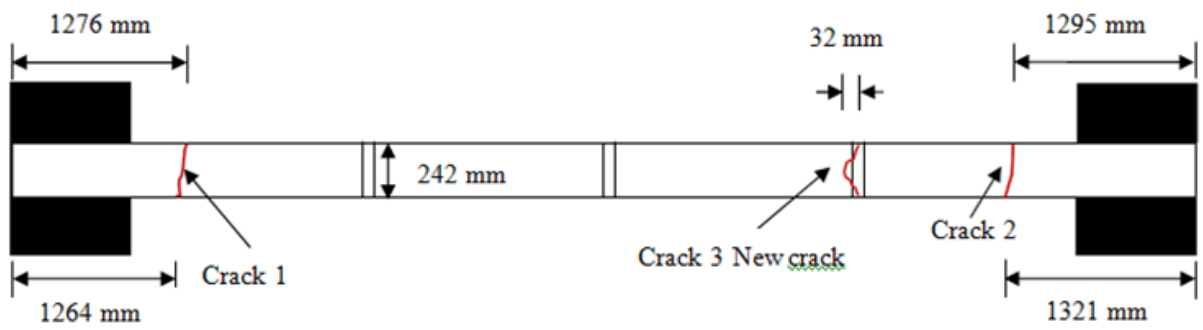
Table 8: Values used to predict average crack spacing and final average crack width.

Panel	L (mm)	t (mm)	Ac (mm ²)	ff (MPa)	db (mm)	Af (mm ²)	Ec (MPa)	Ef (MPa)	f' (MPa)	f*	e * sh
P-2	9144	127	93677	758.4	9.5	168.7	24856	40817	26.6	1.585	-5.10x10 ⁻⁴
P-3	9144	127	76645	758.4	9.5	168.7	24856	40817	26.6	1.602	-5.15x10 ⁻⁴
P-4	9144	127	51097	758.4	9.5	168.7	24856	40817	26.6	1.641	-5.25x10 ⁻⁴
P-5	9144	127	38323	758.4	9.5	168.7	24856	40817	26.6	1.678	-5.33x10 ⁻⁴
P-6	9144	127	30677	758.4	9.5	168.7	24856	40817	26.6	1.712	-5.41x10 ⁻⁴

The maximum crack widths measured for panels P-1 through P-6 in the initial (at 203 days), second (at 762 days) and final studies (at 2400 days) are shown in Table 7. Figure 8 & 9 illustrate the comparisons of the final average crack widths and maximum crack widths from panel P-1 to panel P-6 at the different stages of inspection.

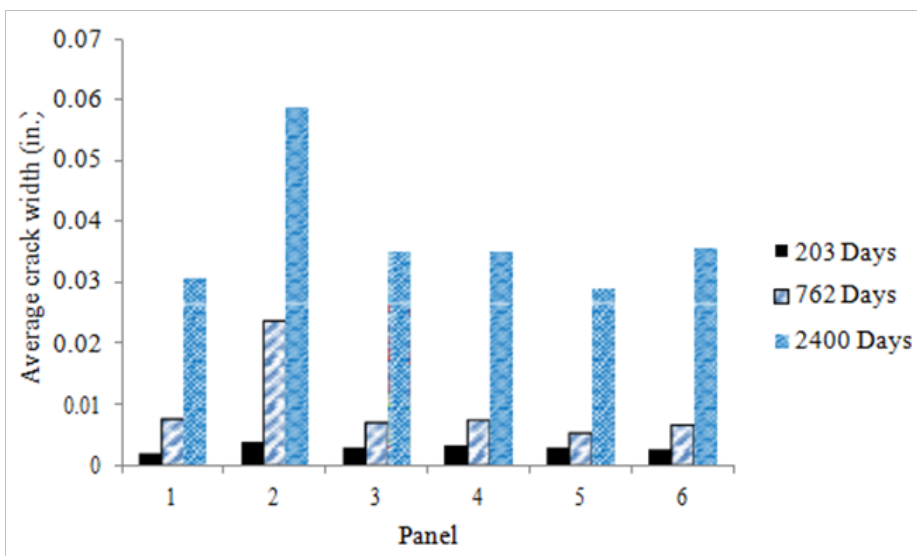
From Tables 6 & 7, panel P-1 (steel, =0.18%) shows the final average and maximum crack widths increase of 1463% and 1383% from original measurement to ultimate value respectively. The final average and maximum crack widths in panel P-2 (GFRP, =0.18%) have increased 1390% and 920%

in ultimate study stage respectively. Panel P-3 (GFRP, =0.22%) has an average crack width 1086% and a maximum crack width 1176% when comparing ultimate measurement with initial result. Panel P-4 (GFRP, =0.33%) illustrates the ultimate average crack and maximum cracking value have increased 970% and 831% respectively. The increases of the final average and maximum crack width in panel P-5 (GFRP, =0.44%) are 880% and 719% respectively. Average crack width in panel P-6 (GFRP, =0.55%) has increased 1257%, and the maximum crack width increases 1490% in final measurement. Therefore, it can be concluded that the rate of crack width development is the lowest in panel P-5.



Conversion Units: 1in. = 25.4mm

Figure 7: Panel P-6 (GFRP, $\rho = 0.55\%$).



Conversion Units: 1in. = 25.4mm

Figure 8: Comparison of total average crack widths.

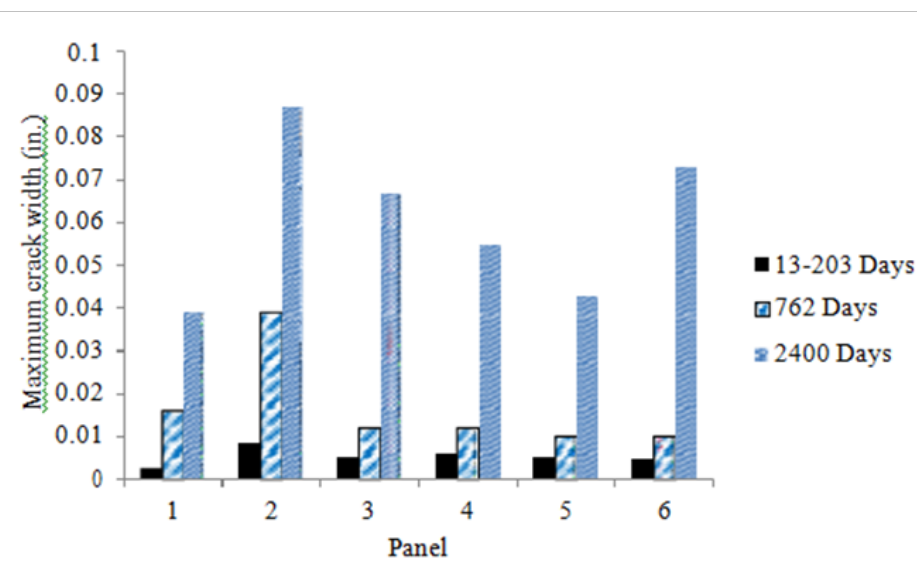


Figure 9: Comparison of maximum crack widths.

According to the Figure 7 through 8, the final average crack width and maximum crack width are the smallest in panel P-5 (GFRP, $\rho=0.44\%$) at 2400 days when the panels are reinforced with GFRP bars. This can illustrate that the reinforcement ratio of panel P-5 may be a reasonable shrinkage and temperature one.

In addition, it should be noted that crack widths increase constantly with time. It may be explained (1). GFRP bars are susceptible to attack under exposures to moisture, alkaline solutions and elevated temperature. In addition, it is well known that the coefficients of thermal expansion (CTE) of FRP bars are different in the longitudinal and transverse directions. The longitudinal CTE, depending on fibers, is lower than that of concrete, while the transverse CTE, depending on matrix, is about 3-6 times larger than that of concrete [22]. GFRP can experience an expansion of 4-6 times greater than that of concrete in the transverse direction due to temperature variations. As a result, an increase in temperature produces bursting stresses within the concrete surrounding the reinforcement, which may cause splitting cracks or de-bonding of bars from concrete. This fact involves a degradation of the bond between concrete and reinforcement, affecting the structural response [23]. Moreover, under freezing-thawing cycles, ice formation at the interface between FRP and concrete leads to further loss of the FRP bond to concrete and increase existing crack width under sustained loads [24]. Additionally, volume changes may result in material fatigue and de-bonding of reinforcement due to repetitive shrinkage and swelling when the concrete surrounding GFRP bars subject to wetting-drying conditions in the vicinity of the main crack [25,26]. These appear as micro-cracks generally naked to the eye. Their stiffness will decrease greatly. In addition, cracks are the easiest location for moisture and aggressive chemicals to accelerate the deterioration of reinforcement as well as to reduce the service life of concrete structures [21]. The cracks on the panels extended through the height and width of the panels. This creates more exposed surface areas leading to increased shrinkage and creep over several years. Therefore, the crack width will be bigger and bigger with time. (2). The fixed-fixed end supports of these panels, which provide the restraint to shrinkage, are not immovable, but are adjacent parts of the structure that are themselves prone to shrinkage. If the exterior supports of the panels produce a relative movement, at the same time, these panels also create drying shrinkage that is restrained by exterior supports. As a result, the crack width increases gradually. (3). Due to the self-weight (sustained load) of these panels, which cannot be ignored even if flexural cracking cannot be induced by self-weight directly because of the larger cracking moment compared to moments caused by self-weight for these panels; the moment and shear stresses are maximum values at the exterior restrained supports and interior roller supports on these panels that can also contribute.

Theoretical versus experimental results

There are limited studies that predict cracking characteristics especially long-term cracking behaviors including average crack

width and average crack spacing of fully restrained concrete deck slabs reinforced with GFRP bars, and stress distribution in reinforcing bars at cracking locations due to restrained drying shrinkage. Gilbert [1] analyzed shrinkage cracking characteristics of a direct tension concrete member reinforced with steel bars that were fully restrained and developed theoretical formulas to estimate the crack spacing and final average width of fully restrained concrete slab by using equations (1), (2), (3), and (4)

$$S_0 = \frac{d_b}{10\rho} \quad (1)$$

where S_0 is that stresses in concrete and reinforcing bars are no longer affected directly by the presence of this crack, d_b is the bar diameter, ρ is the reinforcement ratio. The final tensile force, $N(\infty)$ due to shrinkage and temperature changes was given by

$$N(\infty) = -\frac{n^* A_s}{C_2} (\sigma_{av} + \varepsilon_{sh}^* E_e^*) \quad (2)$$

Where $n^* = E_s/E_e^*$, A_s is the area of reinforcement, σ_{av} is estimate of the average concrete stress in the period after first cracking, $(\sigma_{c1} + f_t)/2$, σ_{c1} is concrete stress away from the crack when occurring first crack, $N_c/(1+C_1)/A_c$, $C_1 = 2s_0/(3L-2s_0)$, L is the length of member, f_t is the tensile strength of concrete, ε_{sh}^* is the final shrinkage strain, E_e^* is final effective modulus for concrete, $E/(1+\phi^*)$, ϕ^* is the final creep coefficient, $C_2 = 2s_0/(3L-2s_0)$, S is crack spacing by expressed as

$$s \leq \frac{2s_0(1+\xi)}{3\xi} \quad (3)$$

$$\text{where } \xi = \frac{-n^* \rho (\sigma_{av} + \varepsilon_{sh}^* E_e^*)}{n^* \rho (\sigma_{av} + \varepsilon_{sh}^* E_e^*) + f_t}$$

$$w = -\left[\frac{\sigma_{c1}^*}{E_e^*} \left(s - \frac{2}{3} s_0 \right) + \varepsilon_{sh}^* S \right] \quad (4)$$

where w is the final average crack width, σ_{c1}^* is final concrete stress away from the crack, $N(\infty)(1+C_1)/A_c \leq f_t$.

In this model, the longitudinal movement of reinforced concrete member that is caused by changes of temperature and drying shrinkage of concrete is restrained by fully fixed-fixed end supports. These equations were proposed by Gilbert based on concrete slab reinforced with steel bars. Some factors, therefore, should be investigated and modified for FRP-reinforced members. Ghatefar et al. [20,21] studied early-age restrained shrinkage cracking of concrete deck slabs reinforced with GFRP bars. They modified the coefficient of S_0 that was used by Gilbert's model on each side of the crack. Finally, they predicted reasonably average crack spacing and crack width by using the modified S_0 and Gilbert's model. In this paper, the Gilbert's model was used. The coefficients for S_0 and S were modified and calibrated according to the experimental results. In order to evaluate the average crack width and cracking spacing for each panel by using Gilbert analytical model, ACI 209.2R-08

[27] guideline was used to determine ultimate shrinkage strain (ϵ_{sh}^*) and ultimate creep coefficient (ϕ^*). Table 8 illustrates the parameters that were used to predict the final average crack width and average crack spacing.

At the crack location, the reinforcing bars completely carried the direct tension force due to shrinkage and temperature changes because crack that extended the full width of the panel and propagated over the full depth of the panel. The distance S_0 , over which the concrete and reinforcing bars stresses vary considerably in the region adjacent to the crack, needs to be known. It was proposed originally by Favre et al. [28] for a concrete member reinforced with deformed steel bars or welded wire mesh. Nejadi and Gilbert [5] found that S_0 may be calculated using Eq. (1) at first cracking. However, this value of S_0 should be multiplied by a coefficient of 1.33 for final or long-term calculation. Ghatefar et al. [20] revised this coefficient. It was varied from 0.1 to 1.6 in 0.1 increments until a reasonable agreement. They obtained a coefficient of 0.8.

Two coefficients of 1.33 and 0.8 that were considered as the coefficient value for S_0 in this paper resulted in substantial differences between experimental results and theoretical calculations. The value, therefore, was adjusted from 0.1 to 1.0 in 0.01 increments for each panel. However, it was noted that average cracking spacing for each panel caused still high inconsistency between experimental and analytical results. The coefficient values for S_0 and s were varied simultaneously from 0.1 to 1.0 in 0.01 increments until relatively small errors were obtained. These adjusted values were regressed to obtain the regression equations for α and β . It was concluded that these equations were related to reinforcement ratios of each panel. The regression equation of coefficient value α for S_0 was expressed as:

$$\alpha = \frac{1}{-993.4\rho + 6.708} \quad (5)$$

where α is coefficient of S_0 , ρ is reinforcement ratio. It was found that coefficient value (β) for s kept a constant of value of 0.95, which yielded reasonable agreement between experimental results and theoretical predictions, when the reinforcement ratios of these panels was equal to or more than 0.0044. Therefore, The regression equation of coefficient value (β) of panels P-2, P-3, P-4, and P-5 for was given by:

$$\beta = 232.04\rho - 0.0746 \quad (6)$$

where β is coefficient of s . This value for panel P-6 was 0.95. Table 9 illustrates the coefficients of each panel that were adjusted and regressed for S_0 and S .

Table 10 provides a comparison between the final crack width calculated by using the coefficients of α and β and final average crack width measured in ultimate study period. Average crack spacing using β adjusted is illustrated Table 11. Table 10

shows that the measured crack widths due to shrinkage and temperature changes for panel P-2, P-4, P-5, and P-6 agree with the values of theoretical prediction based on Gilbert's model [1] with an error that is less than 25% error except panel P-3. The difference between experimental and analytical values of crack width for panel P-3 may be resulted from an error of measurement or a contingency because there is only one panel for each type of panels. Comparisons between the experimental data and results predicted by theoretical model for average crack spacing of these panels are illustrated in Table 11. The measured average crack spacing for each panel agrees with the value of analytical model with the largest error of 22%.

Table 9: Panel coefficients of each panel for S_0 and S .

Panel	ρ	Coefficient for s_0	α	Coefficient for s	β
P-2	0.0018	0.2	0.203	0.34	0.343
P-3	0.0022	0.21	0.221	0.44	0.436
P-4	0.0033	0.28	0.292	0.69	0.691
P-5	0.0044	0.45	0.428	0.95	0.95
P-6	0.0055	0.8	0.804	0.95	0.95

Table 10: Final average crack widths.

	P-2	P-3	P-4	P-5	P-6
Theoretical (mm)	1.85	1.28	0.99	0.82	0.97
Experimental (mm)	1.49	0.89	0.89	0.73	0.91
Percentage (%)	24.17	43.62	11.29	10.94	6.43

Table 11: Average crack spacing.

	P-2	P-3	P-4	P-5	P-6
Theoretical (cm)	361	344	339	387	446
Experimental (cm)	449	441	431	448	419
Percentage (%)	19.62	22.07	21.24	13.5	6.43

Conclusion

The main purpose of this study was to investigate long-term shrinkage cracking behavior in fully restrained concrete panels reinforced with GFRP bars. One reinforced concrete panel and five GFRP panels with end-restrained supports were experimented under field environment in Rolla, Missouri for seven years (2400 days). Gilbert's model that was initially proposed for concrete members reinforced with steel bars was applied to GFRP concrete panels to estimate crack behavior. Suggested modifications to the two coefficients for s_0 and s were proposed for GFRP panels. According to experimental data and theoretical predictions in this research, the following conclusions can be drawn:

- a. As axial restraining forces induced by the restrained shrinkage and temperature changes of these concrete

panels caused the highest level of tensile stress at the exterior support of the panel; in addition, the distributed moment and shear stresses were maximum values at the restrained concrete supports and interior roller supports on these panels. The cracks appeared at or near exterior or intermediate supports. When comparing the cracking moments with maximum positive and negative moments caused by self-weight for these panels as illustrated in Table 5, the cracking moments were greater. The restrained shrinkage, therefore, should be a major factor to induce crack for each panel.

b. Panel P-5 was observed that the average and maximum crack width increased 880% and 719% respectively when comparing with the results of original measurement. These increasing percentages of panels P-5 are the lowest among the GFRP panels.

c. When comparing the measured average shrinkage crack width and cracking spacing for each GFRP panel with the results that were calculated by using Gilbert modified analytical model, the errors for average crack width and cracking spacing were within 22% respectively. This was accomplished by modifying the coefficients of s_0 and s that were related to reinforcement ratio of GFRP panel. However, the coefficient for s should be 0.95 after reinforcement ratio reached 0.0044. The error is comparable to the error found by both Gilbert (steel reinforced RC) and Ghatifar et al. (GFRP reinforced RC) in their early-age studies, however, this work was undertaken over a much longer seven year period of study and presents refined factors for later-age cracking using GFRP reinforcement.

References

- Gilbert RI (1992) Shrinkage cracking in fully restrained concrete members. *ACI Structural Journal* 89(2): 141-149.
- Branham N, Myers JJ (2006) Secondary reinforcement requirements for concrete reinforced with GFRP. Report Number 06-65. University of Missouri-Rolla.
- American Concrete Institute (2011) Building code requirements for structural concrete and commentary. ACI 318-11, Detroit.
- American Concrete Institute (2006) Guide for the Design and Construction of Concrete Reinforced with FRP Bars. ACI 440.1R-06, Farmington Hills, MI.
- Nejadi S, Gilbert I (2004) Shrinkage cracking and crack control in restrained reinforced concrete members. *ACI Structural Journal* 101(6): 840-845.
- Krauss PD, Rogalla EA (1996) Transverse cracking in newly constructed bridge decks. NCRP Rep. No.380, Transportation Research Board Business Office, National Research Council, Washington, DC.
- Frosch RJ, Blackman DT, Radabaugh RD (2003) Investigation of bridge deck cracking in various bridge superstructure systems. Joint Transportation Research Program, E-por No: FHWA/IN/JTPP-2002/25, Indian Depat. Of Transportation and Purdue University, West Lafayette, IN.
- ISIS Canada (2006) Durability of fiber reinforced polymers in civil infrastructure. The Canadian Network for Centers of Excellence on Intelligent Sensing for Innovative Structures (ISIS), Durability Monograph, Winnipeg, MB, Canada.
- Golden C, Myers JJ (2007) Investigation of Long-Term Crack Patterns in FRP and Steel Reinforced Concrete Panels. Undergraduate Research. University of Missouri-Rolla.
- Japan Concrete Institute (1999) Technical Committee on Autogenous Shrinkage of Concrete "Committee Report". Autogenous Shrinkage of Concrete. In: Tazawa EE, Spon FN (Eds.), London, p. 1-67.
- Mindess S, Young JF, Darwin D (2003) Concrete (2nd edn). Prentice-Hall, Upper Saddle River, NJ.
- Byard BE, Schindler AK, Barnes RW, Rao A (2010) Cracking Tendency of Bridge Deck Concrete. *Journal of the Transportation Research Board* 2164: 122-131.
- Chen RH, Choi JH (2002) Effects of GFRP reinforcing rebars on shrinkage and thermal stresses in concrete. Proc 15th ASCE Engineering Mechanics Conf, Columbia Univ, New York, USA, p. 1-8.
- Gilbert RI (2001) Shrinkage, cracking and deflection the serviceability of concrete structures. *Electronic Journal of Structural Engineering* 1(1): 2-14.
- Qiao PZ, McLean ID, Zhang JM (2010) Mitigation strategies for early-age shrinkage cracking in bridge decks. Research Report WA-RD 747.1, Washington State Transportation Center, Washington State University, Olympia, WA.
- Xi Y, Shing B, Xie Z (2001) Development of Optimal Concrete Mix Designs for Bridge Decks. Report No. CDOT-DTD-R-2001-11, sponsored by the Colorado Department of Transportation.
- Folliard KJ, Smith CA, Sellers JG, Brown MD, Breen JE (2003) Evaluation of Alternative Materials to Control Drying Shrinkage Cracking in Concrete Bridge Decks. Research Report 0-4098-4, Center for Transportation Research, University of Texas at Austin, Austin, TX.
- Delatte N, Mack E, Cleary J (2007) Evaluation of High Absorptive Materials to Improve Internal Curing of Low Permeability Concrete. State Job Number 134227, Final Report, Cleveland State University, Cleveland, OH.
- Nejadi S, Gilbert RI (2003) Shrinkage cracking in fully-restrained reinforced concrete members. UNICIV Report, School of Civil and Environmental Engineering, University of New South Wales, Sydney, Australia.
- Ghatifar A, El-Salakawy E, Bassuoni MT (2014) Effect of reinforcement ratio on transverse early-age cracking of GFRP-RC bridge deck slabs. *Journal of Composites for Construction*, ASCE 18(6): 1-9.
- Ghatifar A, El-Salakawy E, Bassuoni MT (2015) Early-age restrained shrinkage cracking of GFRP-RC bridge deck slabs: Effect of environmental conditions. *Cement and Concrete Composites* 64(2015): 62- 73.
- Gentry TR (1996) Thermal compatibility of plastic composite reinforcement and concrete. *Advanced composite materials in bridges and structures*. Montreal, Que.: Canadian Society for Civil Engineering, pp. 149-156.
- Tepfers R (1979) Cracking of concrete cover along anchored deformed reinforcing bars. *Mag Concr Res* 31 (106): 3-12.
- Ales J, El-Ragaby A, El-Salakawy E (2011) Durability of GFRP bars bond to concrete under different loading and environmental conditions. *Journal of Composites for Construction*, ASCE 15(3): 249-269.

25. Ayano T, Wittmann FH (2002) Drying, moisture distribution, and shrinkage of cement-based materials. *Journal of Materials and Structures* 35(3): 134-140.
26. Zhang J, Gao Y, Han Y, Sun W (2012) Shrinkage and interior humidity of concrete under dry-wet cycles. *Int J Dry Technol* 30(6): 583-596.
27. American Concrete Institute (2008) *Guide for Modeling and Calculating Shrinkage and Creep in Hardened Concrete*. ACI 209.2R-08, Farmington Hills, MI.
28. Favre R (1983) *Fissuration et Deformations*. Manual du Comite Euro-International du Beton (CEB), Ecole Polytechnique Federale de Lausanne, Switzerland, pp. 249.



This work is licensed under Creative Commons Attribution 4.0 License
DOI: [10.19080/CERJ.2018.04.555648](https://doi.org/10.19080/CERJ.2018.04.555648)

**Your next submission with Juniper Publishers
will reach you the below assets**

- Quality Editorial service
- Swift Peer Review
- Reprints availability
- E-prints Service
- Manuscript Podcast for convenient understanding
- Global attainment for your research
- Manuscript accessibility in different formats
(Pdf, E-pub, Full Text, Audio)
- Unceasing customer service

Track the below URL for one-step submission
<https://juniperpublishers.com/online-submission.php>